Veterinary Microbiology 294 (2024) 110125

Contents lists available at ScienceDirect

Veterinary Microbiology

journal homepage: www.elsevier.com/locate/vetmic

Engineering and characterizing porcine reproductive and respiratory syndrome virus with separated and tagged genes encoding the minor glycoproteins

Minze Zhang, Bang Qian, Michael Veit *

Free University Berlin, Faculty of Veterinary Medicine, Institute of Virology, Robert von Ostertagstr 7, Berlin 14163, Germany

ARTICLE INFO

Keywords:
PRRSV
Gp2
Gp3
Gp4
Overlapping genes
Separation of genes
Tagged gene

ABSTRACT

Porcine reproductive and respiratory syndrome virus (PRRSV) is a major pathogen affecting pigs and belongs to the enveloped plus-stranded RNA virus family Arteriviridae. A unique feature of Arteriviruses is that the genes encoding the structural proteins overlap at their 3` and 5` ends. This impedes mutagenesis opportunities and precludes the binding of short peptides for antibody detection, as this would alter the amino acids encoded by the overlapping gene. In this study, we aimed to generate infectious PRRSV variants with separated genes encoding the minor glycoproteins Gp2, Gp3, and Gp4, accompanied by appended tags for detection. All recombinant genomes facilitate the release of infectious virus particles into the supernatant of transfected 293 T cells, as evidenced by immunofluorescence of infected MARC-145 cells using anti-nucleocapsid antibodies. Furthermore, expression of Gp2-Myc and Gp3-HA was confirmed through immunofluorescence and western blot analysis with tag-specific antibodies. However, after two passages of Gp2-Myc and Gp3-HA viruses, the appended tags were completely removed as indicated by sequencing the viral genome. Recombinant viruses with separated Gp2 and Gp3 genes remained stable for at least nine passages, while those with Gp3 and Gp4 genes separated reverted to wild type after only four passages. Notably, this virus exhibited significantly reduced titers in growth assays. Furthermore, we introduced a tag to the C-terminus of Gp4. The Gp4-HA virus was consistently stable for at least 10 passages, and the HA-tag was detectable by western blotting and immunofluorescence.

1. Introduction

Arteriviruses are a family of enveloped positive-sense RNA viruses that includes the porcine reproductive and respiratory syndrome virus (PRRSV) and the equine arteritis virus (EAV). Distinct PRRSV genotypes were identified in Europe (Lelystad virus) and North America (VR-2332) in the early 1990 s, but meanwhile the viruses have spread worldwide, and new viruses continuously emerge, including highly virulent ones. Because of the low nucleotide identity, PRRSV is now classified as two species, PRRSV-1 (European type) and PRRSV-2 (American type) (Benfield et al., 1992; Kuhn et al., 2016; Meulenberg et al., 1993b).

Arteriviruses contain seven structural proteins: the nucleocapsid protein N and six membrane proteins, the glycoproteins Gp2, Gp3, Gp4, that are supposed to form a heterotrimeric complex, Gp5, which is disulfide-linked to M, and the small E-protein. N, M and Gp5 are major virion components, whereas E, Gp2, Gp3 and Gp4 are referred to as minor structural proteins. The function of the seventh membrane protein, ORF5a, is unclear, but it is required for efficient replication in cell culture (Dokland, 2010; Snijder et al., 2013; Veit et al., 2014).

From reverse genetics experiments with EAV and PRRSV it is known that all structural proteins seem to be essential for virus replication. If either Gp5 or M are deleted from the viral genome, no virus particles are released from infected cells. Thus, Gp5 and M are required for virus budding, but an additional function during virus entry cannot be excluded. If expression of either Gp2 or Gp3 or Gp4 is abrogated, virus particles bud from cells, but the particles are not infectious indicating that cell entry is disturbed in the absence of the minor glycoprotein complex (Wieringa et al., 2004; Wissink et al., 2005). Furthermore, exchange of ectodomains of Gp2/3/4, but not those of Gp5 and M, between PRRSV and EAV alters cell tropism of the resulting recombinant viruses, reinforcing the notion that the minor glycoprotein complex is required for cell entry (Dobbe et al., 2001; Verheije et al., 2002). Interestingly, the E protein, a myristoylated hydrophobic protein, that might function as an ion channel, interacts either physically or

* Corresponding author.
E-mail address: Michael.Veit@fu-berlin.de (M. Veit).

https://doi.org/10.1016/j.vetmic.2024.110125
Received 15 March 2024; Received in revised form 13 May 2024; Accepted 18 May 2024
Available online 21 May 2024

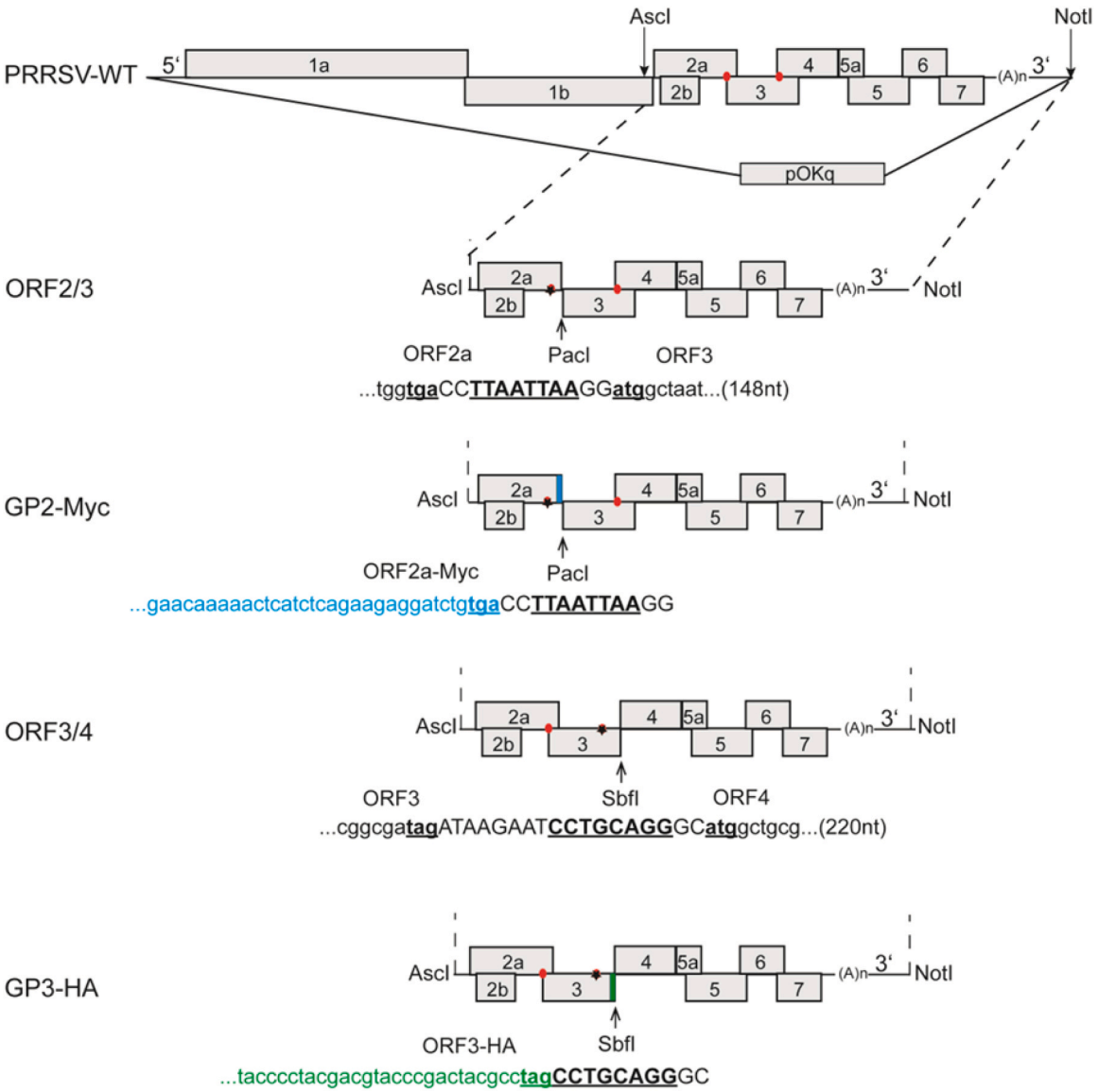

Fig. 1. Schematics to create recombinant virus. The genomic structure of full-length PRRSV-2 cDNA clone. ORFs 1a and 1b encode the polyproteins from which the non-structural proteins are derived. ORF 2a, 2b, 3, 4, 5a, 5, 6 and 7 encode the structural proteins Gp2, E, Gp3, Gp4, ORF5a, Gp5, M and N, respectively. The fragment indicated by stippled lines was cut out at two naturally occurring restriction sites and used as template for subsequent gene manipulation. The start codons of ORF3 and ORF4 (red dots) were first mutated silently and then unique restriction sites (indicated by arrows), either *Pac*I or SbfI were inserted downstream of the stop codon. The sites were used to insert the missing nucleotides including a start codon of the downstream gene and to insert a Myc- or HA-tag to the C-terminus of Gp2 and Gp3, respectively. A part of the modified nucleotide sequences are depicted below the schematics. The start (atg) and stop codons (tag or tga) are underlined and bold, the restriction sites are underlined and bold capitalized and the nucleotides encoding the Myc- and HA-tag are coloured blue and green, respectively.

functionally with the Gp2/3/4 complex. Its deletion from the EAV genome completely prevents incorporation of Gp2/3/4 into virus particles (Du et al., 2010; Thaa et al., 2009; Wieringa et al., 2004).

Gp5 comprises an N-terminal cleavable signal peptide, followed by an ectodomain containing several N-glycosylation sites. The following hydrophobic region spans the membrane three times and the C-terminus is hydrophilic and located in the cytosol. M has the same folding, but lacks a signal peptide and is not glycosylated (de Vries et al., 1995a; Snijder et al., 2003; Veit et al., 2022). Gp2 and Gp4 are typical type I membrane proteins with a cleavable N-terminal signal peptide, a relatively short ectodomain, one transmembrane region and a short cytoplasmic tail (de Vries et al., 1995b; Wieringa et al., 2003; Wieringa et al., 2002). Gp3 has a similar primary structure (N-terminal signal peptide and one hydrophobic region), but our work with Gp3 of EAV and PRRSV provided evidence that it exhibits an unusual hairpin-like topology. Both the N-terminus and C-terminus are exposed to the lumen of the ER and an internal hydrophobic region peripherally anchors the protein to membranes (Matczuk et al., 2013; Matczuk and Veit, 2014; Zhang et al., 2018).

The Arterivirus structural proteins are encoded by seven open reading frames (ORFs), named ORF2a (Gp2), ORF 2b (E), ORF3 (Gp3), ORF 4 (Gp4), ORF5a, ORF5 (gp5), ORF6 (M) and ORF 7 (N) (de Vries et al., 1992; Wissink et al., 2003). They are translated from subgenomic mRNAs, which are generated by a discontinuous transcription mechanism. This creates a nested set of transcripts, which are 3′coterminal and contain a common 5` leader sequence, which is derived from the genomic 5′end (Fang and Snijder, 2010; Gorbalenya et al., 2006). Discontinuous transcription is governed by transcription-regulating sequences (TRSs), one TRS is downstream of the leader sequence and the others (called body TRS) at the 3′ end of each open reading frame (de Vries et al., 1990). As the polymerase moves along the genome to make a negative-stranded copy, it encounters one body TRS, where it might

undergo a template-switching event. This allows the polymerase to jump from the body TRS to the leader TRS, where transcription continues resulting in the synthesis of subgenomic RNAs. Since they are negative-stranded they must be subsequently copied into positive-stranded RNA to function as mRNAs (Pasternak et al., 2006; van Marle et al., 1999).

Although TRSs are characterized by conserved hexanucleotide motifs, this motif varies between arteriviruses. [UCAAC(U/C)] is the leader TRS in EAV (den Boon et al., 1996), while [UUAACC] in all PRRSV strains of both species. In contrast, the body TRSs are more diverse: [U/A/G][U/A/G][A/C][A/G][C/U]C among PRRSV-2 strains, and U [A/U/C][A/G][A/C]CC among PRRSV-1 strains (Meulenberg et al., 1993a; Tan et al., 2001). The sequence of the TRS as well as the distance between the TRS site and the following start codon affects the expression of the respective ORF (Faaberg et al., 1998; Meulenberg et al., 1993a; Nelsen et al., 1999; Wang et al., 2017).

Furthermore, most structural proteins of Arteriviruses are encoded by overlapping genes: In the genome of PRRSV-2 ORF2b encoding the E-protein is completely present inside ORF2. The 3` end of ORF2, as well as most other ORFs encoding the other structural proteins, are overlapping with the 5´end of the following ORFs. An exception is ORF4 of PRRSV-2; its stop codon is ultimately preceded by the start codon of ORF5a and separated by further nucleotides from the start codon of ORF5 (Firth et al., 2011).

In this study, we delineate our efforts to segregate the ORF2, ORF3, and ORF4 genes of a PRRSV-2 virus and subsequently attach a tag to the C-terminus of the smaller glycoproteins. These tags serve as valuable tools for analysing virus replication in cell culture, given the scarcity of available antibodies that also only interact with closely related virus strains. Moreover, these tags, upon integration into a vaccine and elicitation of an antibody response, have the potential to distinguish between animals that are infected and those that have been vaccinated.

2. Methods

2.1. Cells, virus and expression plasmid

The cell lines 293 T (Human embryonic kidney cells) and MARC-145 (simian kidney epithelial cells derived from MA-104) were maintained as adherent culture in Dulbecco's Modified Eagle's Medium (DMEM) (PAN, Aidenbach, Germany) supplemented with 10% fetal calf serum (FCS), 100 U of penicillin and 100 mg of streptoMycin per ml at 37C in an atmosphere with 5% CO2 and 95% humidity.

PRRSV virus strain: XH-GD, Chinese highly pathogenic PRRSV-2 strain, accession number EU624117.1, which was rescued from the infectious cDNA clone pPRRSV-WT as described below.

Expression plasmid: ORF4 encoding Gp4 amplified from the infectious cDNA clone pPRRSV-WT was cloned into the plasmid pCAGGS, which contains a synthetic CAG promoter, composed of three elements, (C) the cytomegalovirus (CMV) early enhancer element, (A) the first exon and the first intron of the chicken beta-actin gene and (G) the splice acceptor of the rabbit beta-globin gene. The C-terminus of Gp4 was fused via a small linker (PV) to a Myc-tag consisting of the amino acids EQKLISEEDL.

Cells in 6-well plates were transfected with 2.5 µg plasmid DNA using Lipofectamine 3000 (Thermo Fisher Scientific, Carlsbad, United States) as described by the manufacturer.

2.2. Generation of mutant PRRSV genomes

The pPRRSV-WT full-length infectious cDNA clone, generously provided by Prof. Guihong Zhang from South China Agricultural University, was derived from the PRRSV-2 virus XH-GD strain (GenBank accession no. EU624117) (Zhang et al., 2013). The complete PRRSV-2 genome is harboured in the plasmid pok-Q, featuring a CMV promoter and a terminal BGH RNA transcription terminator sequence. The genes encoding structural proteins were excised from the genome using the *Asc*I and *Not*I restriction enzymes and served as templates for mutagenesis and insertion through overlap extension polymerase chain reaction (PCR) (Veit et al., 2008).

Multiple steps were necessary to generate the mutants illustrated in Fig. 1. In the case of the ORF2/3 mutant, the initial step was to eliminate the start codon of ORF3 with the mutation ATG to GTG which does not alter the encoded amino acid in Gp2. To achieve separation of ORF2 and ORF3 a nucleotide sequence containing a unique *Pac*I restriction site was first inserted downstream of the ORF2a stop codon which allows the insertion of the 148-nt overlap between ORF2a and ORF3 in a second mutagenesis step. For construction of the Gp2-Myc mutant, the nucleotide sequences encoding a Myc tag (EQKLISEEDL) were appended to the C-terminus of Gp2 in the ORF2/3 mutant with the *Pac*I restriction site. Mutants ORF3/4 or Gp3-HA were generated using a similar strategy. The start codon of ORF4 was first silently mutated. To achieve separation of ORF3 and ORF4 a nucleotide sequence containing a unique SbfI restriction site plus the 220-nt overlap between ORF3 and ORF4 was inserted downstream of the ORF3 stop codon. For construction of the Gp3-HA mutant, the nucleotide sequences encoding a HA-tag (YPYDVPDYA) was fused to the C-terminus of Gp3 in the ORF3/4 mutant with the SbfI restriction site. As a result, all four recombinant genomes contain the overlapping nucleotide sequence twice, but in the first part the start codon was inactivated.

To generate the Gp4-HA mutant a nucleotide sequence encoding a HA tag (YPYDVPDYA) was fused to the C-terminus of Gp4, since the ORF4 gene does not overlap with the downstream ORF5a and ORF5 genes. The authenticity of the resulting plasmids was verified by sequencing and the genes encoding the structural proteins were subsequently inserted into the plasmid pok-Q to generate recombinant virus.

2.3. Generation of recombinant PRRS virus

The plasmids (2.5 µg) containing the complete PRRSV genome from wildtype and mutants were transfected into 80% confluent 293 T cells grown in 6-well plates using Lipofectamine 3000 (Thermo Fisher Scientific, Carlsbad, United States) as described by the manufacturer. 72 hours after transfection the supernatant (=P0 virus) was removed and cleared by low speed centrifugation, 500 µl was used to infect MARC-145 cells grown to 70–80% confluency on 6-well plates. After incubation for 1.5 h at 37C, the inoculums were removed, cells were washed twice with PBS, and further incubated in culture medium (DMEM with 2% FCS) for 72 h. Cells were then subjected to immunofluorescence assay using anti-N of PRRSV-2 monoclonal antibody. The supernatant collected from infected MARC-145 cells was defined as P1 virus. The nucleotide sequence of rescued viruses was analysed by Sanger-sequencing of a PCR-product encompassing the mutation and insertion site.

2.4. SDS-PAGE, Western blot and Glycosidase digestion

After sodium dodecyl sulfate-polyacrylamide gel electrophoresis (SDS-PAGE) using 12% polyacrylamide, gels were blotted onto polyvinylidene difluoride (PVDF) membranes (GE Healthcare, Freiburg im Breisgau, Germany). After blocking of membranes (blocking solution: 5% skim milk powder in PBS with 0.1% Tween-20 (PBST)) for 1 h at room temperature, the primary antibodies listed above were applied overnight at 4C: After washing (3×10 min with PBST), the horseradish peroxidase-coupled secondary antibodies listed above were applied for 1 hour at room temperature. After washing, signals were detected by chemiluminescence using the ECLplus reagent (Pierce/Thermo, Bonn, Germany) and a Fusion SL camera system (Peqlab, Erlangen, Germany).

To analyze Endo H resistance of Gp4, MARC-145 cell transfected with the expression plasmid encoding Gp4-Myc, or infected with recombinant Gp4-HA virus as well as virus pellets prepared from the supernatant of infected cells were lysed in glycoprotein denaturing buffer

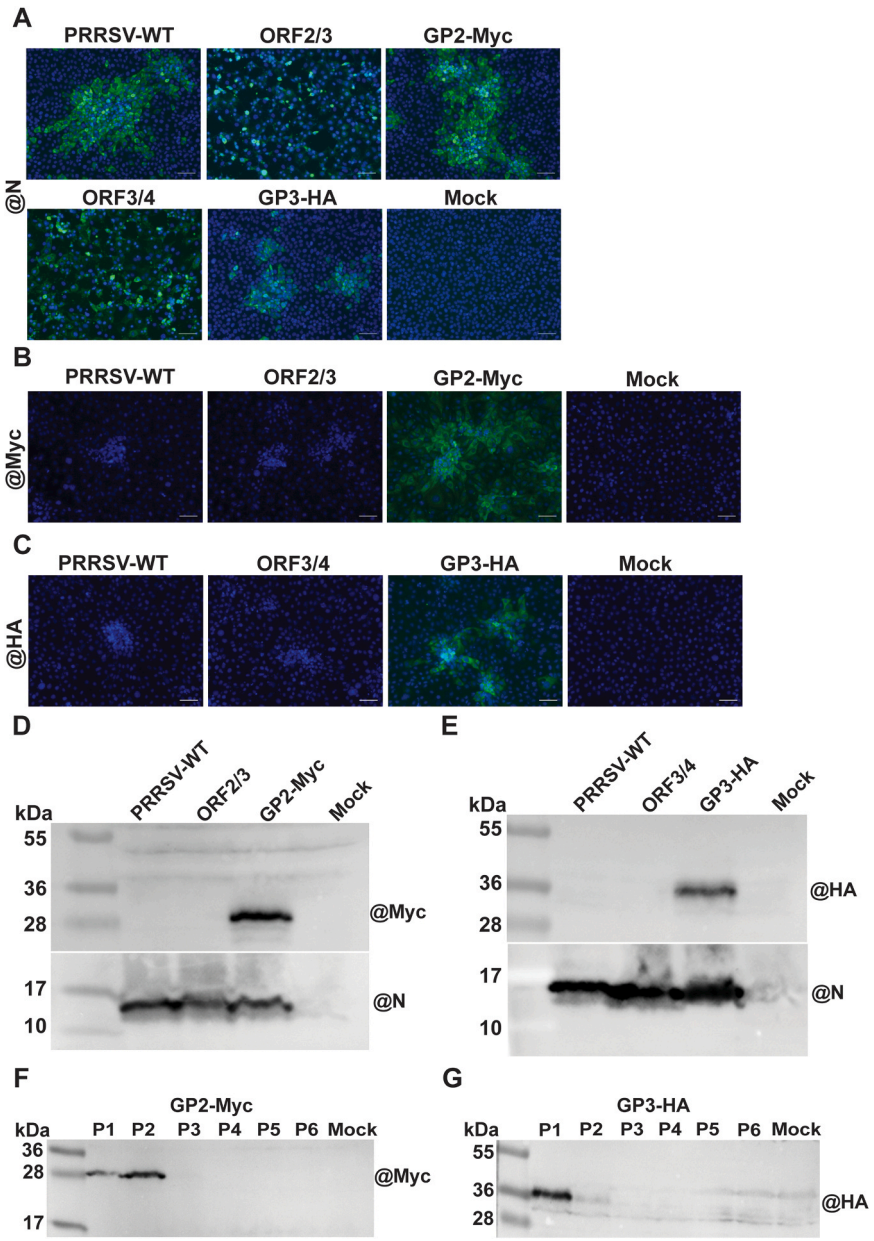

Fig. 2. Characterization of recombinant virus. A-C. The supernatant of HEK-293 T cells (=P0 virus) transfected by the indicated cDNA clones of PRRSV-2 was used to infect Marc-145 cells. Upon the appearance of a cytopathic effect (72 h p. i.) cells were permeabilized and stained, either with anti-N monoclonal antibody (@N) and Alexa Fluor 488 anti-mouse secondary antibody (A) or with anti-Myc (@Myc) antibodies (B) or anti-HA (@HA) antibodies (C) and Alexa Fluor 488 anti-rabbit secondary antibodies. Nuclei were stained with DAPI in A, B and C. Mock: uninfected cells. Scale bar, 100 μm. **D, E.** Supernatant of 293 T cells transfected with the indicated cDNA clones of PRRSV-2 (=P0 virus) were used to infect Marc-145 cells. Upon the appearance of a cytopathic effect (72 h p.i.), cells were lysed and subjected to SDS-PAGE and Western blotting with anti-Myc (D) or anti-HA (E) antibodies. Staining of the same membrane with anti-N monoclonal antibodies served as the infection control. **F, G.** The P0 virus was serially passaged 6 times in Marc-145 cells. At each passage a CPE was visible after 2–3 days. An aliquot of the resulting supernatants was used to infect Marc-145 cells, upon the appearance of a cytopathic effect (72 h p.i.), cells were lysed and subjected to SDS-PAGE and Western blotting with anti-Myc (F) or anti-HA (G) antibodies.

(0.5% SDS, 40 mM DTT), boiled for 10 min at 100C and an aliquot was digested either with endobeta-N-acetyl-glucosaminidase (Endo H, 2.5–5units/μL, 4 h at 37C) or Peptide-N-Glycosidase (PNGase F, 2.5–5units/μL, 4 h at 37C) according to the manufacturer's instruction (New England Biolabs, Frankfurt am Main, Germany). Deglycosylated or untreated samples were supplemented with reducing SDS-PAGE loading buffer and subjected to SDS-PAGE and Western blot.

2.5. Immunofluorescence and confocal microscopy

Transfected or infected MARC-145 cells grown in 6-well or 24-well plates were washed twice with PBS, fixed with paraformaldehyde (4% in phosphate-buffered saline (PBS)) for 15 min at room temperature, washed twice with PBS, permeabilized with 0.2% Triton in PBS for 10 min at room temperature, and washed again twice with PBS. After blocking (blocking solution: 3% bovine serum albumin (BSA) in PBS with 0.1% Tween-20 (PBST)) for 30 min at room temperature, the cells were incubated with the primary antibodies listed above for one hour at room temperature. After washing three times with PBS, cells were incubated with the secondary antibodies listed above. Pictures were recorded using a ZEISS Axio Vert. A1 inverse epifluorescence microscope or Leica Stellaris 8 FALCON confocal microscope.

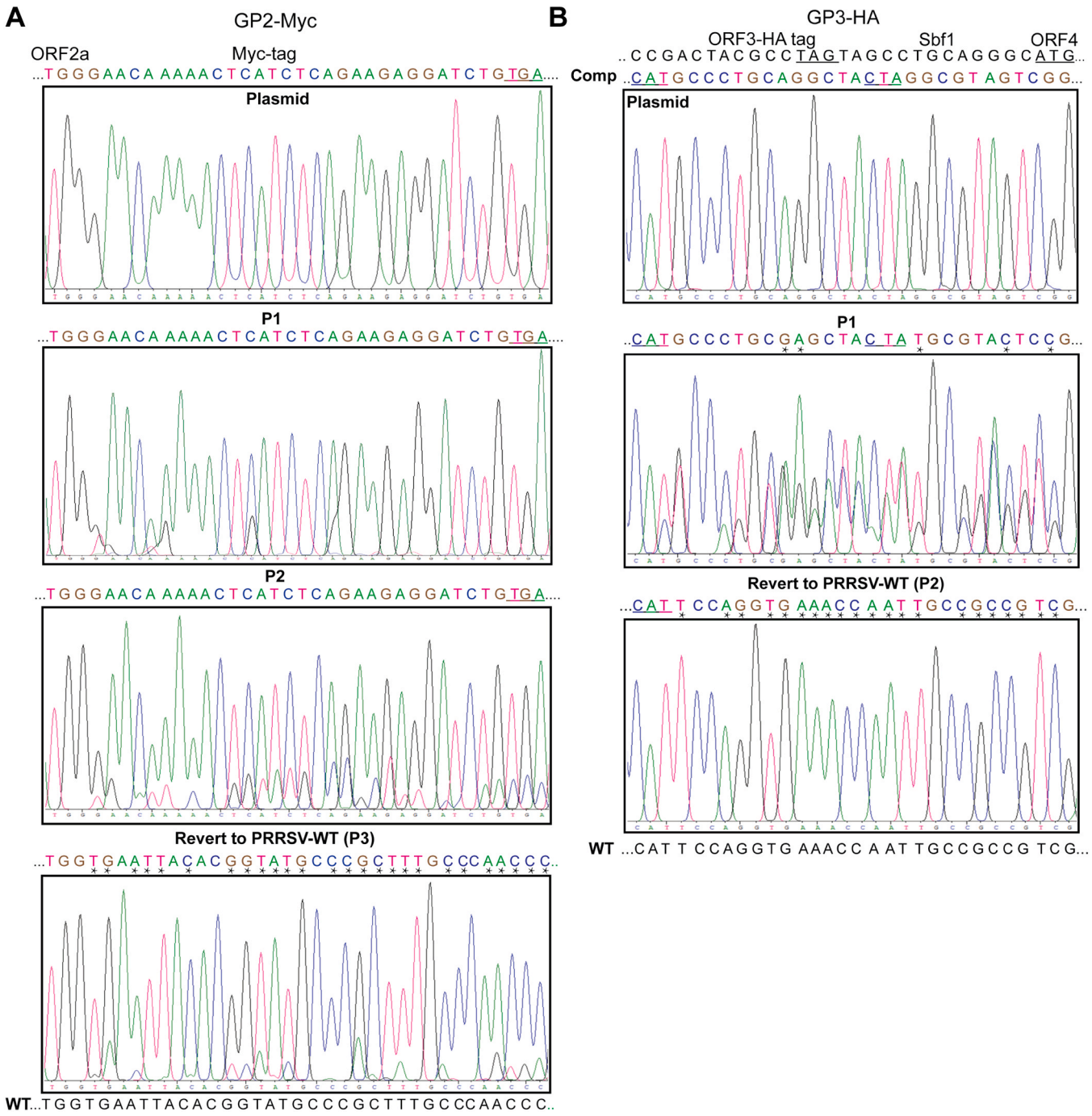

Fig. 3. Genomic instability of Gp2-Myc and Gp3-HA virus. The supernatant harvested from Marc-145 cells (=P1 virus) infected with Gp2-Myc and Gp3-HA virus was serially passaged 5 times. Viral RNA was isolated from supernatants, subjected to RT-PCR and the manipulated gene region was sequenced. (A) The sequencing chromatograms covering the Myc-tag from the plasmid containing the full-length viral genome, P1, P2 and P3 virus of Gp2-Myc are shown. (B) The sequencing chromatograms covering part of HA-tag, restriction site SbfI and start codon of ORF4 from the plasmid, P1 and P2 virus of Gp3-HA are shown. The consensus sequence is depicted above the sequencing chromatograms. The start codon (ATG) and stop codon (TGA) are underlined. The asterisks (·) indicate when a substituted nucleotide forms the dominant peak. Wt is the sequence of the wild-type virus before the mutagenesis. Gp2-Myc was sequenced with a forward primer and hence the sequence shown corresponds to the coding, positive-sense RNA. Gp3-HA was sequenced with a reverse primer and hence the sequence shown corresponds to the non-coding, negative-sense RNA. In that case the reverse complement of the sequenced nucleotides is shown above.

2.6. Determination of the viral growth kinetics

Sub-confluent MARC-145 cells in 24-well plates were infected with recombinant viruses (P1) at a multiplicity of infection (MOI) of 0.01. After 1.5 h incubation at 37℃, cells were washed three times with PBS and incubated at 37℃ in 0.5 ml DMEM containing 2% FCS in a CO^2 incubator. At certain time points (12, 24, 36, 48, 60, 72, 84 and 96 h) post-infection, supernatants were collected and frozen at −80℃ until use. The viral titres were determined in MARC-145 cells with the tissue culture infection dose 50% endpoint assay ($TCID_{50}$).

2.7. Preparation of PRRSV particles

MARC-145 cells grown in three T-175 flasks were infected with

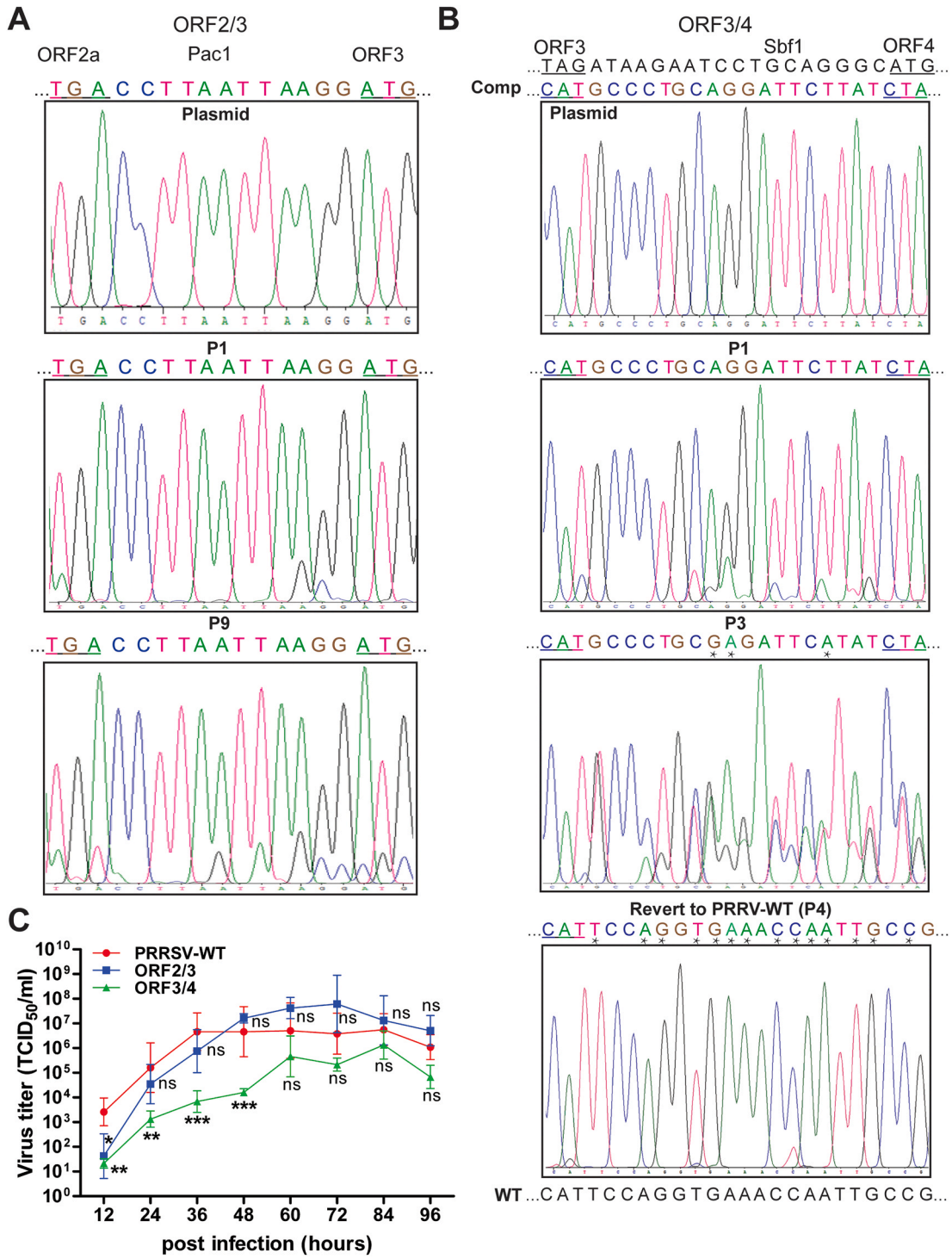

Fig. 4. Genomic instability of ORF2/3 and ORF3/4 virus. Supernatant harvested from Marc-145 cells (=P1 virus) infected with ORF2/3 and ORF3/4 virus were serially passaged 8 times (P1-P9). At each passage a CPE was visible after 2–3 days. Viral RNA was isolated from P1-P9 virus and subjected to RT-PCR and the manipulated gene region was sequenced. **A.** The sequencing chromatograms covering the stop codon TGA of ORF2a, the *Pac*I restriction site and the start codon ATG of ORF3 from the plasmid, P1 and P9 virus of ORF2/3 are shown. **B.** the sequencing chromatograms covering the stop codon of ORF3, the restriction site SbfI and start codon of ORF4 from plasmid, P1, P3 and P4 virus of ORF3/4 are shown. The consensus sequence is depicted above the sequencing chromatograms. The start codon (ATG) and stop codon (TGA) are underlined. The asterisks (·) indicate when a substituted nucleotide forms the dominant peak. ORF2/3 was sequenced with a forward primer and hence the sequence shown corresponds to the coding, positive-sense RNA. ORF3/4 was sequenced with a reverse primer and hence the sequence shown corresponds to the non-coding, negative-sense RNA. In that case the reverse complement of the sequenced nucleotides is shown above. **C.** Growth kinetics of ORF2/3 and ORF3/4 virus. Marc-145 cells in 24-well plates were infected with PRRSV at a MOI of 0.01. Culture supernatants were collected at the indicated time points and titers were determined with a $TCID_{50}$ assay. The geometric mean titers with standard deviations (error bars) from three independent infections are shown. The asterisks indicate statistically significant differences (*P<0.05, **P<0.01, ***P<0.001) at the same time point between PRRSV-WT and mutants. Two-way ANOVA followed by Bonferroni post-test was applied for comparing replicates means.

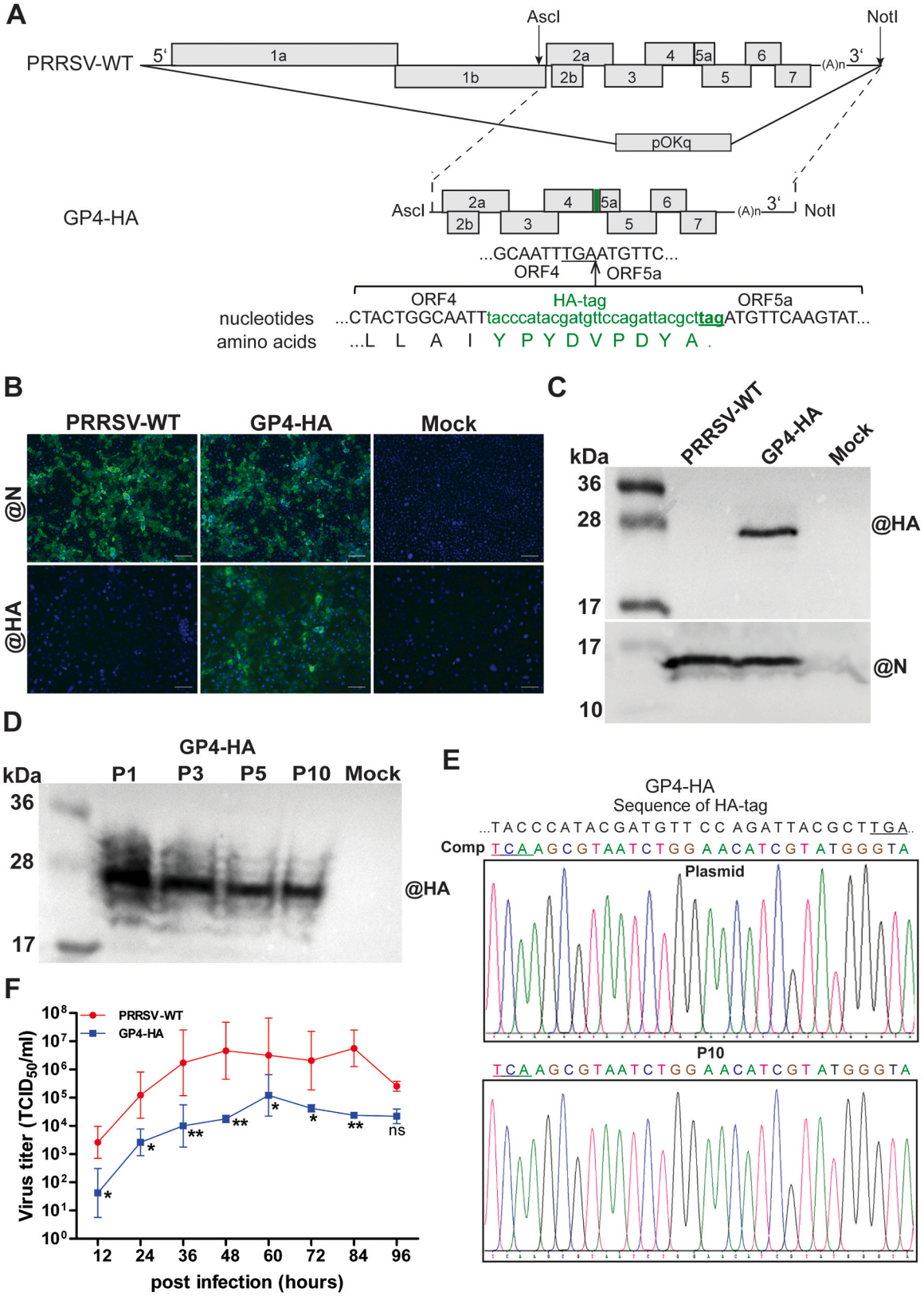

(caption on next page)

Fig. 5. Generation and characterizing Gp4-HA virus. A. Schematic presentation of construction of infectious cDNA clone of Gp4-HA virus. **B+C.** Detection of Gp4 in Marc-145 cells infected with Gp4-HA virus. (B) Supernatant of 293 T cells transfected with the indicated cDNA clones of PRRSV-2 (=P0 virus) were used to infect Marc-145 cells. Upon appearance of a cytopathic effect (72 h p. i.), cells were permeabilized and stained either with anti-N monoclonal antibody or anti-HA antibodies, and nuclei with DAPI, or (C) were lysed and subjected to SDS-PAGE and Western blotting with anti-HA antibodies. Staining of the same membrane with anti-N antibodies served as the infection control. **D.** The lysates of cells infected with from P1, P3, P5 and P10 Gp4-HA virus were subjected to SDS-PAGE and Western blotting with anti-HA antibodies. Mock: uninfected cells. The apparent molecular masses in kDa are shown on the left side of each blot. **E.** Sequencing P1 and P10 virus of recombinant Gp4-HA. Supernatant harvested from infected Marc-145 cells (=P1 virus) by Gp4-HA virus were serially passaged 9 times (P1-P10). Viral RNA was isolated from P1 and P10 virus of recombinant Gp4-HA virus and subjected to RT-PCR. The manipulated gene region was sequenced with a reverse primer and hence the sequence shown corresponds to the non-coding, negative-sense RNA. In that case "Comp" is the reverse complement of the sequenced nucleotides. The stop codon (TGA) is underlined. **F.** Growth kinetics of Gp4-HA virus. Marc-145 cells in 24-well plates were infected with PRRSV at a MOI of 0.01. Culture supernatants were collected at the indicated time points and titers were determined with a $TCID_{50}$ assay. The geometric mean titers with standard deviations (error bars) from three independent infections are shown. The asterisks indicate statistically significant differences (*P<0.05, **P<0.01, ***P<0.001) at the same time point between PRRSV-WT and mutants. Two-way ANOVA followed by Bonferroni post-test was applied for comparing replicates means.

PRRSV mutant Gp4-HA at a multiplicity of infection (MOI) of 0.01 and incubated for 3–4 days at 37℃ in DMEM until cytopathic effects became visible. Cell culture supernatants were harvested, cleared by low-speed centrifugation (3000 g, 30 min) and applied on top of a sucrose cushion (20% w/v in TNE buffer (10 mM Tris-HCl, 10 mM NaCl, 1 mM EDTA, pH 7.5)). Samples were ultracentrifuged for 2 h at 28,000 rpm at 4℃ in a Beckman SW32 rotor. The virus pellet was resuspended in TNE buffer and frozen at −80℃ until use.

2.8. Statistical analysis

Data are expressed as means ± standard deviations. The significance of the variability among

experiments was determined by paired t-test as specified in the figure legends using GraphPad Prism (version 5.0) software.

3. Results

3.1. Creation of recombinant virus with separated ORF2, ORF3, and ORF4 genes and tagged Gp2 and Gp3

Creation of recombinant PRRSV-2 virus with separated genes involved several steps. We started with a full-length cDNA of the Chinese PRRSV-2 strain XH-GD cloned into a plasmid downstream of the cytomegalovirus (CMV) immediate-early (IE) promotor to construct a genome where ORF2, ORF3 and ORF4 were separated and each of the minor glycoproteins Gp2, Gp3, and Gp4 individually fused at their C-termini with short tags (Myc or HA), facilitating subsequent protein detection and analysis. To achieve this, we employed naturally occurring restriction sites *Asc*I and *Not*I in the cDNA to excise a fragment encompassing the genes encoding all structural proteins up to the 3′ end of the genome. This fragment allows the subsequent gene modification (Fig. 1).

To create the required mutations and insertions between ORF2 and ORF3, we utilized overlap extension PCR mutagenesis. Initially, we silently mutated the original start codon of Gp3, followed by the introduction of the unique restriction site *Pac*I after the stop codon of Gp2. The *Pac*I site was used to insert the missing 148 nucleotides encoding the N-terminus of Gp3 including a new start codon thereby ensuring the expression of authentic Gp3 protein. Additionally, we utilized the *Pac*I site to add a Myc-tag to the C-terminus of Gp2, providing a means of detecting and monitoring this protein.

The same strategy was employed to separate ORF3 and ORF4 while introducing an HA-tag at the C-terminus of Gp3. The transcription regulating sequences (TRS) were left untouched in each construct, but the distance between the TRS and the start codon and hence the length of the 5′untranslated region of the resulting sgRNA increased by 148 and 220 nucleotides, respectively.

3.2. The viruses with separate genes and tagged Gp2 and Gp3 revert back to the wild-type sequence after a few passages

To assess the functionality of the generated recombinant viruses, subgenomic cDNAs were cloned back into the full-length cDNA clone, which was transfected into HEK-293 T cells. 48 hours after transfection the cell culture supernatant was removed and an aliquot was used to inoculate MARC-145 cells. Immunofluorescence with antibodies against the nucleocapsid protein N revealed that all constructs were capable of producing infectious virus particles (Fig. 2a). This P1 virus, derived from the initial transfection, exhibited expression of Gp2-Myc and Gp3-HA, as evidenced by immunofluorescence (Fig. 2b-c) and western-blotting analysis (Fig. 2d-e) with anti-Myc and anti-HA antibodies, respectively.

To investigate the genomic stability of the introduced mutations, the recombinant viruses were passaged six times in MARC-145 cells, which showed at each passage a strong cytopathogenic effect around day two or three p. i. indicating virus replication. MARC-145 cells were infected with cell culture supernatant from each passage and subjected to western blotting with anti-Myc or anti-HA antibodies. The P1 and P2 virus is able to express Gp2-Myc and Gp3-HA, respectively. However, in subsequent passages (P3 and onwards), the expression of tagged glycoproteins was no longer detectable, indicating a loss of the tag sequences during early viral passages (Fig. 2f-g).

Sequencing of the viral genome in the region where the tags were introduced showed their presence in the plasmid used for genome manipulation. However, in the P3 Gp2-Myc virus and P2 Gp3-HA virus, the tag sequences were completely absent, and the sequences matched those from wild-type viruses without separated genes. The viruses from the intervening passages showed a gradual reversion to the wt sequence. The consensus sequence of P1 Gp2-Myc virus was the same as that of the plasmid, but reversion to the wt sequence was already seen at single nucleotides. The frequency of reversion progressed in P2 Gp2-Myc virus and was almost completed in the P3 virus (Fig. 3a). A similar, but faster process was seen for the Gp3-HA virus, the P1 virus exhibits that some nucleotides already reverted to wt and reversion was completed in the P2 virus (Fig. 3b). Note, that one passage corresponds to several replication cycles since the cells were infected with a low multiplicity of infection of 0.01.

Motivated by these results, we asked how stable the viruses with the separated genes are. We passaged them up to nine times in MARC-145 cells and sequenced the resulting viruses. The ORF2/3-separated virus maintained sequence integrity up to passage 9, at least as far as the consensus sequence is concerned, indicating higher stability. Double peaks are seen in the P1 virus at two nucleotides, and the number of nucleotides affected increases during subsequent virus passage, but the nucleotides introduced by us are still predominant in the P9 virus (Fig. 4a). On the other hand, the ORF3/4 separated viruses showed in some nucleotides dominant reversions back to the wild-type sequence after only three passages that were fully completed after the fourth passage, suggesting less stability in comparison (Fig. 4b).

To compare the growth characteristics of the PRRSV wild-type (wt) with the ORF2/3 and ORF3/4 separated mutants, we generated a

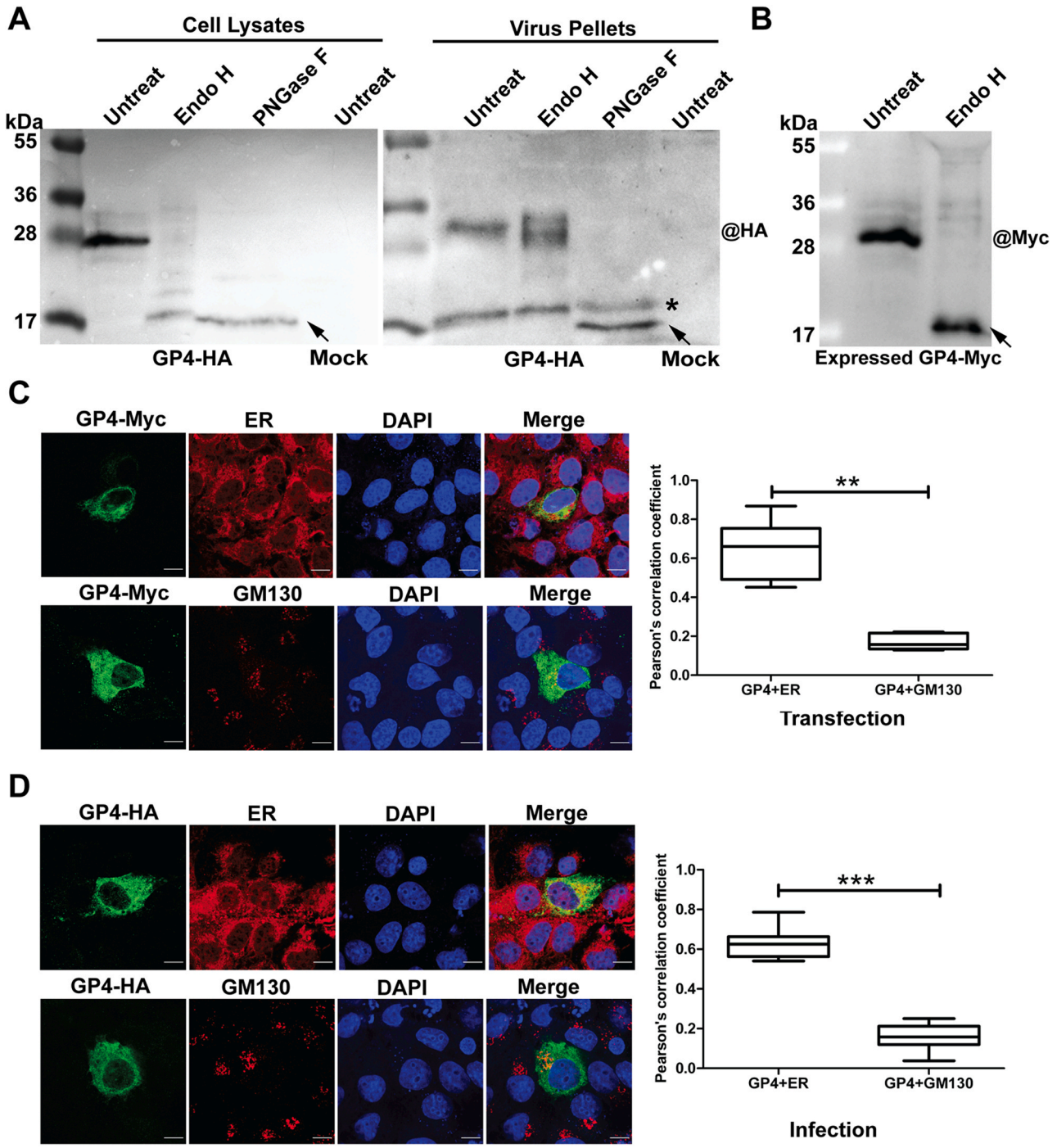

Fig. 6. Intracellular transport of Gp4-HA in infected Marc-145 cells. A. Endo H resistance of Gp4 in infected Marc-145 cells. Marc-145 cells infected with recombinant Gp4-HA virus were lysed at 48 h p. i. (Cell lysates on left panel) and virus particles were purified from supernatant. (Virus pellets on right panel) Samples were either treated with Endo H, PNGase F or untreated prior to reducing SDS-PAGE and Western blot with anti-HA antibodies. **B.** Endo H resistance of Gp4 in expressed Marc-145 cell. Marc-145 cells transfected with Gp4-Myc expression plasmid were lysed at 48 h p.i., either treated with Endo H or left untreated prior to reducing SDS-PAGE and Western blot with HA antibodies. Asterisk (·) indicated the unspecific band, Arrowhead pointed the deglycosylated Gp4 from digestion either by Endo H or PNGase F. **C.** Gp4 in expressed Marc-145 cells localized in ER. Marc-145 cells were transfected with Gp4-Myc, Gp4 was stained with monoclonal antibodies against the Myc-tag followed by secondary anti-mouse antibodies coupled to Alexa Fluor-488, Cis-Golgi was stained with polyclonal anti-GM130 antibodies followed by secondary anti-rabbit antibodies coupled to Alexa Fluor-568 and nuclei with DAPI. ER was stained directly with Red fluorescence-Cytopainter from Abcam. Scale bar: 10 μm. **D.** Gp4 in infected Marc-145 cells also localized in ER. Marc-145 cells were infected with Gp4-HA virus, Gp4 was stained with monoclonal antibodies against the HA-tag followed by secondary anti-mouse antibodies coupled to Alexa Fluor-488, Cis-Golgi was stained with polyclonal anti-GM130 antibodies followed by secondary anti-rabbit antibodies coupled to Alexa Fluor-568 and nuclei with DAPI. ER was stained directly with Red fluorescence-Cytopainter from Abcam. At least 40 cells were quantified with the Pearson's correlation coefficient method using the JACoP plugin of the ImageJ software. The asterisks indicate statistically significant differences (*P < 0.05, * * P < 0.01, * * * P < 0.001) between groups. Paired t-test was applied for statistical analysis. Scale bar: 10 μm.

growth curve using P1 viruses where gene separation was still present. MARC-145 cells were infected at a low multiplicity of infection (m.o.i), and the virus titers were monitored at various time points. PRRSV wt reached its highest titer of 10E7 already at 36 hours post-infection (p.i.). Titers remained stable until 60 h p.i. and thereafter titers started to decline, likely due to thermal inactivation of the viruses over time. Titers of ORF2/3 separated mutants are one to two logarithms lower at early time points, identical to wt virus after 36 hours, and continue to rise until 72 hours post infection before slowly dropping. In contrast, the ORF3/4 separated mutants exhibited different growth dynamics, indicating their distinct biological properties. Titers are lower than PRRSV wt by up to four logs at almost all time points, reaching the highest titers only after 84 hours. The slower growth kinetics and lower titers exhibited by the ORF3/4 separated mutants inherently explain their more rapid reversion towards the wild-type sequence compared to the ORF2/3 separated mutants (Fig. 4c).

3.3. PRRS virus with an HA-tag fused to the C-terminus of Gp4 is stable

Finally, we produced a mutant genome in which the C-terminus of Gp4 was HA-tagged. Since ORF4 does not overlap with the following genes ORF5a or ORF5 in PRRSV-2, the sequence encoding the HA-tag could be inserted by PCR mutagenesis without any preparatory steps (Fig. 5a). As with the other constructs, the transfection of these modified genomes into 293 T cells resulted in the release of infectious viruses. This was confirmed by both immunofluorescence assays and Western blotting, employing anti-HA antibodies for detection (Fig. 5b+c). Serially passaging the supernatant of transfected 293 T cells in MARC-145 cells, we found that the expression of Gp4-HA remained robustly detectable even after the tenth passage (Fig. 5d). Moreover, the viral genome displayed no indications of reversion to the wild-type sequence (Fig. 5e). Although the genome of Gp4-HA virus is stable, the virus shows marked growth inhibition in MARC-145 cells. At every time-point of the growth curve, the titers of the Gp4-HA virus were two to three logarithms lower than those of the PRRSV-wt (Fig. 5f).

3.4. Processing and intracellular transport of Gp4 in transfected and infected cells

We then used the Gp4-HA virus to study the processing and intracellular transport of Gp4-HA. Marc-145 cells were infected with the Gp4-HA virus, the supernatant was removed 48 h p. i., virus particles were pelleted and lysed. The remaining cells were also lysed and an aliquot of both lysates was treated with either PNGase F to remove all N-linked carbohydrates, with Endo-H to remove immature carbohydrates, or was left untreated. SDS-PAGE and western blotting showed that the largest fraction of intracellular Gp4-HA has a molecular weight of 27 kDa and was almost completely sensitive against Endo-H digestion. Only a very small faction of Gp4-HA is larger and apparently Endo-H resistant (Fig. 6a). The same band pattern was seen when Gp4 fused in a similar manner to a Myc-tag was expressed in the absence of the other viral proteins (Fig. 6b). In contrast, Gp4-HA in virus particles exhibits a larger molecular weight of 32 kDa which is Endo-H resistant (Fig. 6a). This indicates that Gp4-HA remains in an intracellular compartment proximal to the medial Golgi where glycoproteins acquire Endo-H resistance. This compartment was identified by confocal microscopy using markers for the ER and the cis-Golgi. In transfected cells, Gp4-Myc showed a reticular staining pattern characteristic for the ER. It also co-localizes strongly with the ER-marker, but not with the cis-Golgi marker (Fig. 6c). An identical staining and co-localization pattern were seen in virus-infected cells (Fig. 6d).

We conclude that the overwhelming majority of Gp4-HA localizes to the ER, not only in transfected but also in infected cells. Since Gp4-HA in virus particles is Endo-H resistant, but no Endo-H resistant Gp4-HA was detected inside cells we assume that, after budding from the intracellular membrane virus particles are quickly secreted from cells. During this process, the carbohydrates undergo further modifications to attain Endo-H resistance as previously demonstrated for Gp5 (Li et al., 2015).

4. Discussion

Three studies have previously explored the separation of Arterivirus genes that encode major structural proteins, with the aim of introducing tags for antibody or fluorescence detection. In one such study, an HA-tag was attached to the nucleocapsid protein (encoded by ORF7) of a PRRSV-I strain, at either its N- or C-terminus. Although the virus could be rescued, the viability and genetic stability of the recombinant viruses were compromised, leading to the loss of parts of the HA-tag after just four virus passages. However, when additional nucleotides encoding the autoprotease 2 A of foot-and-mouth disease virus were inserted to ensure the generation of a functional N-protein, the HA epitope remained intact after four passages, and the viability of these viruses was not affected (Groot Bramel-Verheije et al., 2000). In two other studies, cDNA clones of a PRRSV-II strain and of EAV were constructed where the ORF4/5, ORF5/6, and ORF6/7 genes were separated, and restriction sites were inserted. The resulting mutant viruses replicated with almost the same efficiency and stably maintained the mutations for up to five passages. However, when the EAV M protein was N-terminally extended by a heterologous sequence, the virus exhibited a clear growth disadvantage compared to the parental virus. Notably, three serial passages did not result in the loss of the foreign genetic material (de Vries et al., 2000; Yu et al., 2009). To date, only one paper has reported the separation of genes for the minor structural proteins of Arteriviruses. In the genome of EAV, ORF3 and ORF4 were separated, and a C-terminal tag was added to Gp3. The recombinant viruses replicated at similar titers to wild-type EAV and were stable until at least passage 9. However, sequence chromatograms of the passage 19 virus showed multiple peaks at various nucleotide positions in the region, indicating that the sequence encoding the tag begins to revert (Matczuk et al., 2019).In another study EGFP was inserted as an independent transcription unit between ORF4 and ORF5a in a PRRSV-2 strain. The resulting recombinant virus grows similarly as wildtype, but the fluorescence was stable for less than 5 passages (Wang et al., 2020).

Most of the recombinant PRRS viruses that we engineered to separate the minor glycoproteins Gp2, Gp3 and Gp4 proved to be even more unstable (Fig. 1). Tags attached to the C-terminus of Gp2 or Gp3 were completely lost after at most two passages in cell culture (Fig. 2+3). Furthermore, even the viruses with separated genes reverted back to the wild type sequence, and lower passages exhibited reduced titers in cell culture (Fig. 3). The reason for the genetic instability and virus viability with attached tags likely lies at the protein level. The tags appear to impair the function of Gp2 and Gp3, such as their efficient interaction with other viral proteins during virus assembly. Similar considerations may also explain the instability and reduced viral replication of the recombinant viruses with tagged proteins described above.

In contrast, it remains unclear why the viruses with the separated genomes are also unstable. The function of overlapping genes is largely unexplored, although they are a common feature in viruses, regardless of their genome type. Most gene overlaps are relatively small, ranging between 10 and 100 nucleotides in length. It has been hypothesized that gene overlapping is widely used by RNA viruses to generate novel genes while maintaining a small genome size. However, mutations in overlapping genes can have a deleterious effect on more than one gene, thereby reducing the evolutionary rate of RNA viruses and their adaptive capacity (Schlub and Holmes, 2020; Simon-Loriere et al., 2013).

These hypotheses might apply to the long-term evolution of viruses in nature, but they do not seem to hold for the replication of PRRSV in cell culture. One speculative explanation is that the increased distance between the transcriptional regulatory sequence (TRS) and the start codon due to the insertion of additional nucleotides, or an altered secondary structure of the resulting subgenomic RNA (sgRNA), may affect the expression rate of the encoded protein. PRRSV uses a tightly

Table 1
Antibodies used in the work.

Application	Target protein	Primary antibody	Secondary antibody
Western Blot	Gp4-Myc	polyclonal anti-Myc tag (16286–1-AP, Proteintech, China, 1:3000)	Anti-rabbit lgG (HRP) (Ab191866, Abcam, UK, 1:5000)
	Gp2-Myc	polyclonal anti-Myc tag (16286–1-AP, Proteintech, China, 1:3000)	
	Gp3-HA	polyclonal anti-HA tag (ab9110, Abcam, UK, 1:5000)	
	Gp4-HA	polyclonal anti-HA tag (ab9110, Abcam, UK, 1:5000)	
	N	monoclonal anti-N of PRRSV-2 (DMAB28442, Creative Diagnostics, USA, 1:3000)	Anti-mouse IgG (HRP) (1706516, Bio-Rad Laboratories, USA, 1:2000)
Immuno-fluorescence	Gp2-Myc	polyclonal anti-Myc tag (16286–1-AP, Proteintech, China, 1:200)	Anti-rabbit IgG coupled to Alexa Fluor 488, Invitrogen, Germany, 1:1000)
	Gp3-HA	polyclonal anti-HA tag (ab9110, Abcam, UK, 1:500)	
	Gp4-HA	polyclonal anti-HA tag (ab9110, Abcam, UK, 1:500)	
	N	monoclonal anti-N of PRRSV-2 (DMAB28442, Creative Diagnostics, USA, 1:1000)	Anti-mouse IgG coupled to Alexa Fluor 488, Invitrogen, Germany, 1:1000)
Confocal microscopy	Gp4-Myc	monoclonal anti-Myc (9B11, Cell signalling technology, Netherland, 1:500)	Anti-mouse IgG coupled to Alexa Fluor 488, Invitrogen, Germany, 1:1000)
	Gp4-HA	monoclonal anti-HA (6E2, Cell signalling technology, Netherland, 1:100)	
	Cis-Golgi Marker	polyclonal anti-GM130 (ab9110, Abcam, UK, 1:500)	Anti-rabbit IgG coupled to Alexa Fluor 568, Invitrogen, Germany, 1:1000)
	ER Marker	stainied directly with Red fluorescence-cytopainter, ab139482, Abcam, UK	

controlled gene expression strategy and disruption of the expression modes of the individual proteins could produce viruses that are inferior in their ability to replicate. (van Marle et al., 1999; Zheng et al., 2014). Table 1

In contrast, a recombinant virus carrying an HA-tag attached to Gp4 exhibited stability over at least 10 passages in cell culture (Fig. 5). However, even this virus displayed compromised growth (Fig. 6). The stability of this mutant might be attributed to the fact that ORF4 does not overlap with the subsequent ORF5a and ORF5 genes (sequence TGA**ATG**TTCAAGT**ATG**). The stop codon of Gp4 (underlined) is ultimately preceded by the start codon of ORF5a (bold) and separated by further nucleotides from the start codon of ORF5 (bold and underlined) (Johnson et al., 2011).

This region of the viral genome and hence the order and overlap between Orf4, Orf5 and Orf5a varies between Arteriviruses. In the PRRSV-1 prototype strain Lelystad and in Lactate Dehydrogenase elevating virus, ORF4 and ORF5 overlap by two nucleotides (underlined) and the start codon of ORF5a (bold) is located two nucleotides downstream (sequence ATGAG**ATG**. In EAV the overlap is more substantial, the start codon of ORF5a and of ORF5 are 31 and 7 nucleotides, respectively upstream of the stop codon of ORF4 (Firth et al., 2011). To introduce a tag, researchers would need to carefully separate the ORF4 and ORF5 genes in these viruses with unknown consequences on genomic stability and efficiency of virus replication.

5. Conclusions

Our study highlights the potential for genetic manipulation of PRRS viruses, but also underscore the challenges in maintaining the viability and genetic stability of recombinant viruses. The successful separation of ORFs encoding the minor glycoproteins and the addition of functional tags without compromising virus viability represents a significant achievement. However, the loss of the sequence encoding the tag added to Gp2 and Gp3 and the reversion to the wild-type sequence in later passages indicates a potential limitation in the long-term stability of these modifications. In contrast, recombinant virus with a HA-tag fused to the C-terminus of Gp4, which does not overlap with the following genes, is stable. Further research is needed to optimize these techniques and fully understand their implications for Arterivirus biology.

Declaration of Generative AI and AI-assisted technologies in the writing processs

During the preparation of this work the authors used Chat GPT 3.5 in order to improve readability and language. After using this tool, the authors reviewed and edited the content as needed and takes full responsibility for the content of the publication.

Funding

This research was funded by the German Research Foundation (DFG, grant no: VE 141/20-1). B.Q. is the recipient of a Ph.D. fellowship from the China Scholarship Council (CSC). The funder played no role in study design, in the collection, analysis and interpretation of data, in the writing of the report, and in the decision to submit the article for publication. We acknowledge support by the Open Access Publication Fund of Freie Universität Berlin.

CRediT authorship contribution statement

Bang Qian: Investigation. **Minze Zhang:** Writing – review & editing, Investigation, Conceptualization. **Michael Veit:** Writing – original draft, Funding acquisition.

Declaration of Competing Interest

All authors declare that they have no conflict of interest regarding the publication of this article.

References

Benfield, D.A., Nelson, E., Collins, J.E., Harris, L., Goyal, S.M., Robison, D., Christianson, W.T., Morrison, R.B., Gorcyca, D., Chladek, D., 1992. Characterization of swine infertility and respiratory syndrome (SIRS) virus (isolate ATCC VR-2332). J. Vet. Diagn. Invest 4, 127–133.

den Boon, J.A., Kleijnen, M.F., Spaan, W.J., Snijder, E.J., 1996. Equine arteritis virus subgenomic mRNA synthesis: analysis of leader-body junctions and replicative-form RNAs. J. Virol. 70, 4291–4298.

Dobbe, J.C., van der Meer, Y., Spaan, W.J., Snijder, E.J., 2001. Construction of chimeric arteriviruses reveals that the ectodomain of the major glycoprotein is not the main determinant of equine arteritis virus tropism in cell culture. Virology 288, 283–294.

Dokland, T., 2010. The structural biology of PRRSV. Virus Res 154, 86–97.

Du, Y., Zuckermann, F.A., Yoo, D., 2010. Myristoylation of the small envelope protein of porcine reproductive and respiratory syndrome virus is non-essential for virus infectivity but promotes its growth. Virus Res 147, 294–299.

Faaberg, K.S., Elam, M.R., Nelsen, C.J., Murtaugh, M.P., 1998. Subgenomic RNA7 is transcribed with different leader-body junction sites in PRRSV (strain VR2332) infection of CL2621 cells. Adv. Exp. Med Biol. 440 275–279.

Fang, Y., Snijder, E.J., 2010. The PRRSV replicase: exploring the multifunctionality of an intriguing set of nonstructural proteins. Virus Res 154, 61–76.

Firth, A.E., Zevenhoven-Dobbe, J.C., Wills, N.M., Go, Y.Y., Balasuriya, U.B., Atkins, J.F., Snijder, E.J., Posthuma, C.C., 2011. Discovery of a small arterivirus gene that overlaps the GP5 coding sequence and is important for virus production. J. Gen. Virol. 92, 1097–1106.

Gorbalenya, A.E., Enjuanes, L., Ziebuhr, J., Snijder, E.J., 2006. Nidovirales: evolving the largest RNA virus genome. Virus Res 117, 17–37.

Groot Bramel-Verheije, M.H., Rottier, P.J., Meulenberg, J.J., 2000. Expression of a foreign epitope by porcine reproductive and respiratory syndrome virus. Virology 278, 380–389.
Johnson, C.R., Griggs, T.F., Gnanandarajah, J., Murtaugh, M.P., 2011. Novel structural protein in porcine reproductive and respiratory syndrome virus encoded by an alternative ORF5 present in all arteriviruses. J. Gen. Virol. 92, 1107–1116.
Kuhn, J.H., Lauck, M., Bailey, A.L., Shchetinin, A.M., Vishnevskaya, T.V., Bao, Y., Ng, T. F., LeBreton, M., Schneider, B.S., Gillis, A., Tamoufe, U., Diffo Jle, D., Takuo, J.M., Kondov, N.O., Coffey, L.L., Wolfe, N.D., Delwart, E., Clawson, A.N., Postnikova, E., Bollinger, L., Lackemeyer, M.G., Radoshitzky, S.R., Palacios, G., Wada, J., Shevtsova, Z.V., Jahrling, P.B., Lapin, B.A., Deriabin, P.G., Dunowska, M., Alkhovsky, S.V., Rogers, J., Friedrich, T.C., O'Connor, D.H., Goldberg, T.L., 2016. Reorganization and expansion of the nidoviral family Arteriviridae. Arch. Virol. 161, 755–768.
Li, J., Tao, S., Orlando, R., Murtaugh, M.P., 2015. N-glycosylation profiling of porcine reproductive and respiratory syndrome virus envelope glycoprotein 5. Virology 478, 86–98.
van Marle, G., Dobbe, J.C., Gultyaev, A.P., Luytjes, W., Spaan, W.J., Snijder, E.J., 1999. Arterivirus discontinuous mRNA transcription is guided by base pairing between sense and antisense transcription-regulating sequences. Proc. Natl. Acad. Sci. USA 96, 12056–12061.
Matczuk, A.K., Chodaczek, G., Ugorski, M., 2019. Production of Recombinant EAV with Tagged Structural Protein Gp3 to Study Artervirus Minor Protein Localization in Infected Cells. Viruses 11.
Matczuk, A.K., Kunec, D., Veit, M., 2013. Co-translational processing of glycoprotein 3 from equine arteritis virus: N-glycosylation adjacent to the signal peptide prevents cleavage. J. Biol. Chem. 288, 35396–35405.
Matczuk, A.K., Veit, M., 2014. Signal peptide cleavage from GP3 enabled by removal of adjacent glycosylation sites does not impair replication of equine arteritis virus in cell culture, but the hydrophobic C-terminus is essential. Virus Res 183, 107–111.
Meulenberg, J.J., Hulst, M.M., de Meijer, E.J., Moonen, P.L., den Besten, A., de Kluyver, E.P., Wensvoort, G., Moormann, R.J., 1993b. Lelystad virus, the causative agent of porcine epidemic abortion and respiratory syndrome (PEARS), is related to LDV and EAV. Virology 192, 62–72.
Meulenberg, J.J., de Meijer, E.J., Moormann, R.J., 1993a. Subgenomic RNAs of Lelystad virus contain a conserved leader-body junction sequence. J. Gen. Virol. 74 (Pt 8), 1697–1701.
Nelsen, C.J., Murtaugh, M.P., Faaberg, K.S., 1999. Porcine reproductive and respiratory syndrome virus comparison: divergent evolution on two continents. J. Virol. 73, 270–280.
Pasternak, A.O., Spaan, W.J.M., Snijder, E.J., 2006. Nidovirus transcription: how to make sense. J. Gen. Virol. 87, 1403–1421.
Schlub, T.E., Holmes, E.C., 2020. Properties and abundance of overlapping genes in viruses. Virus Evol. 6, veaa009.
Simon-Loriere, E., Holmes, E.C., Pagan, I., 2013. The effect of gene overlapping on the rate of RNA virus evolution. Mol. Biol. Evol. 30, 1916–1928.
Snijder, E.J., Dobbe, J.C., Spaan, W.J., 2003. Heterodimerization of the two major envelope proteins is essential for arterivirus infectivity. J. Virol. 77, 97–104.
Snijder, E.J., Kikkert, M., Fang, Y., 2013. Arterivirus molecular biology and pathogenesis. J. Gen. Virol. 94, 2141–2163.
Tan, C., Chang, L., Shen, S., Liu, D.X., Kwang, J., 2001. Comparison of the 5′ leader sequences of North American isolates of reference and field strains of porcine reproductive and respiratory syndrome virus (PRRSV). Virus Genes 22, 209–217.
Thaa, B., Kabatek, A., Zevenhoven-Dobbe, J.C., Snijder, E.J., Herrmann, A., Veit, M., 2009. Myristoylation of the arterivirus E protein: the fatty acid modification is not essential for membrane association but contributes significantly to virus infectivity. J. Gen. Virol. 90, 2704–2712.
Veit, M., Gadalla, M.R., Zhang, M., 2022. Using Alphafold2 to Predict the Structure of the Gp5/M Dimer of Porcine Respiratory and Reproductive Syndrome Virus. Int J. Mol. Sci. 23.
Veit, M., Matczuk, A.K., Sinhadri, B.C., Krause, E., Thaa, B., 2014. Membrane proteins of arterivirus particles: structure, topology, processing and function. Virus Res 194, 16–36.
Veit, M., Ponimaskin, E., Schmidt, M.F., 2008. Analysis of S-acylation of proteins. Methods Mol. Biol. 446 163–182.
Verheije, M.H., Welting, T.J., Jansen, H.T., Rottier, P.J., Meulenberg, J.J., 2002. Chimeric arteriviruses generated by swapping of the M protein ectodomain rule out a role of this domain in viral targeting. Virology 303, 364–373.
de Vries, A.A., Chirnside, E.D., Bredenbeek, P.J., Gravestein, L.A., Horzinek, M.C., Spaan, W.J., 1990. All subgenomic mRNAs of equine arteritis virus contain a common leader sequence. Nucleic Acids Res 18, 3241–3247.
de Vries, A.A., Chirnside, E.D., Horzinek, M.C., Rottier, P.J., 1992. Structural proteins of equine arteritis virus. J. Virol. 66, 6294–6303.
de Vries, A.A., Glaser, A.L., Raamsman, M.J., de Haan, C.A., Sarnataro, S., Godeke, G.J., Rottier, P.J., 2000. Genetic manipulation of equine arteritis virus using full-length cDNA clones: separation of overlapping genes and expression of a foreign epitope. Virology 270, 84–97.
de Vries, A.A., Post, S.M., Raamsman, M.J., Horzinek, M.C., Rottier, P.J., 1995a. The two major envelope proteins of equine arteritis virus associate into disulfide-linked heterodimers. J. Virol. 69, 4668–4674.
de Vries, A.A., Raamsman, M.J., van Dijk, H.A., Horzinek, M.C., Rottier, P.J., 1995b. The small envelope glycoprotein (GS) of equine arteritis virus folds into three distinct monomers and a disulfide-linked dimer. J. Virol. 69, 3441–3448.
Wang, Y., He, W., Li, Q., Xie, X., Qin, N., Wang, H., Huang, J., Lin, S., Ouyang, K., Chen, Y., Huang, W., Wei, Z., 2020. Generation of a porcine reproductive and respiratory syndrome virus expressing a marker gene inserted between ORF4 and ORF5a. Arch. Virol. 165, 1803–1813.
Wang, C., Meng, H., Gao, Y., Gao, H., Guo, K., Almazan, F., Sola, I., Enjuanes, L., Zhang, Y., Abrahamyan, L., 2017. Role of transcription regulatory sequence in regulation of gene expression and replication of porcine reproductive and respiratory syndrome virus. Vet. Res 48, 41.
Wieringa, R., De Vries, A.A., Post, S.M., Rottier, P.J., 2003. Intra- and intermolecular disulfide bonds of the GP2b glycoprotein of equine arteritis virus: relevance for virus assembly and infectivity. J. Virol. 77, 12996–13004.
Wieringa, R., de Vries, A.A., van der Meulen, J., Godeke, G.J., Onderwater, J.J., van Tol, H., Koerten, H.K., Mommaas, A.M., Snijder, E.J., Rottier, P.J., 2004. Structural protein requirements in equine arteritis virus assembly. J. Virol. 78, 13019–13027.
Wieringa, R., de Vries, A.A., Raamsman, M.J., Rottier, P.J., 2002. Characterization of two new structural glycoproteins, GP(3) and GP(4), of equine arteritis virus. J. Virol. 76, 10829–10840.
Wissink, E.H., Kroese, M.V., van Wijk, H.A., Rijsewijk, F.A., Meulenberg, J.J., Rottier, P. J., 2005. Envelope protein requirements for the assembly of infectious virions of porcine reproductive and respiratory syndrome virus. J. Virol. 79, 12495–12506.
Wissink, E.H., van Wijk, H.A., Pol, J.M., Godeke, G.J., van Rijn, P.A., Rottier, P.J., Meulenberg, J.J., 2003. Identification of porcine alveolar macrophage glycoproteins involved in infection of porcine respiratory and reproductive syndrome virus. Arch. Virol. 148, 177–187.
Yu, D., Lv, J., Sun, Z., Zheng, H., Lu, J., Yuan, S., 2009. Reverse genetic manipulation of the overlapping coding regions for structural proteins of the type II porcine reproductive and respiratory syndrome virus. Virology 383, 22–31.
Zhang, M., Cao, Z., Xie, J., Zhu, W., Zhou, P., Gu, H., Sun, L., Su, S., Zhang, G., 2013. Mutagenesis analysis of porcine reproductive and respiratory syndrome virus nonstructural protein 7. Virus Genes 47, 467–477.
Zhang, M., Krabben, L., Wang, F., Veit, M., 2018. Glycoprotein 3 of Porcine Reproductive and Respiratory Syndrome Virus Exhibits an Unusual Hairpin-Like Membrane Topology. J. Virol. 92.
Zheng, H., Zhang, K., Zhu, X.Q., Liu, C., Lu, J., Gao, F., Zhou, Y., Zheng, H., Lin, T., Li, L., Tong, G., Wei, Z., Yuan, S., 2014. Genetic manipulation of a transcription-regulating sequence of porcine reproductive and respiratory syndrome virus reveals key nucleotides determining its activity. Arch. Virol. 159, 1927–1940.